Groundwater

Saltwater Upconing Due to Cyclic Pumping by Horizontal Wells in Freshwater Lenses

by Pieter S. Pauw[1,2,3], Sjoerd E.A.T.M. van der Zee[2], Anton Leijnse[2], and Gualbert H.P. Oude Essink[1,4]

Abstract

This article deals with the quantification of saltwater upconing below horizontal wells in freshwater lenses using analytical solutions as a computationally fast alternative to numerical simulations. Comparisons between analytical calculations and numerical simulations are presented regarding three aspects: (1) cyclic pumping; (2) dispersion; and (3) finite horizontal wells in a finite domain (a freshwater lens). Various hydrogeological conditions and pumping regimes within a dry half year are considered. The results show that the influence of elastic and phreatic storage (which are not taken into account in the analytical solutions) on the upconing of the interface is minimal. Furthermore, the analytical calculations based on the interface approach compare well with numerical simulations as long as the dimensionless interface upconing is below 1/3, which is in line with previous studies on steady pumping. Superimposing an analytical solution for mixing by dispersion below the well over an analytical solution based on the interface approach is appropriate in case the vertical flow velocity around the interface is nearly constant but should not be used for estimating the salinity of the pumped groundwater. The analytical calculations of interface upconing below a finite horizontal well compare well with the numerical simulations in case the distance between the horizontal well and the initial interface does not vary significantly along the well and in case the natural fluctuation of the freshwater lens is small. In order to maintain a low level of salinity in the well during a dry half year, the dimensionless analytically calculated interface upconing should stay below 0.25.

Introduction

Freshwater lenses are important for freshwater supply in coastal areas (Bear et al. 1999; Werner et al. 2013). Pumping from freshwater lenses generally leads to saltwater upconing, that is, a local rise of saline groundwater below the well (Dagan and Bear 1968). As long as saltwater upconing remains limited, freshwater lenses can be sustainably exploited. In case of excessive saltwater upconing, however, there is a high risk of an undesired salinity in the well. Excessive saltwater upconing has led to the closure of wells in many coastal areas (Custodio and Bruggeman 1987; Stuyfzand 1996). Evidently, quantitative analyses on saltwater upconing are important for preventing this type of overexploitation.

Saltwater upconing can be quantified using numerical models or analytical solutions. Analytical solutions for saltwater upconing are mainly based on the interface approach. In this approach, fresh and saline groundwater are separated by an interface and are considered as immiscible fluids with a different density and, in some cases, a different dynamic viscosity. Analytical solutions based on the miscible approach (i.e., based on dispersive solute transport) and variable groundwater density flow are not available due to the mathematical complexity. Using the interface approach, Bower et al. (1999) presented analytical solutions to determine the critical steady-state pumping rate in case of a partially penetrating well in an aquifer overlain by a leaky confining layer. Below the critical pumping rate, the well pumps only fresh groundwater, whereas above the critical pumping rate, the interface below the well has increased above a critical rise, where it is not stable and will rise quickly to the well screen. A steady-state analytical solution to determine the critical pumping rate was also presented by Garabedian (2013) for the case of a partially penetrating well in an aquifer with no-flow conditions at the top and bottom and a constant head boundary condition at a defined radial distance from the well. Zhang et al. (1997) presented an analytical solution for the case of an infinitely long horizontal well in a confined aquifer. Assuming a critical rise of the

[1]Department of Soil and Groundwater, Deltares, P.O. Box 85467, 3508 AL, Utrecht, The Netherlands

[2]Department of Soil Physics and Land Management, Wageningen University, P.O. Box 47, Wageningen, 6700 AA, The Netherlands

[3]Corresponding author: Department of Soil and Groundwater, Deltares, P.O. Box 85457, 3508 AL, Utrecht, The Netherlands; (31) 623786887; pieter.pauw@deltares.nl

[4]Department of Physical Geography, Utrecht University, 3584 CS, Utrecht, The Netherlands

Article impact statement: Applying analytical solutions for quantifying saltwater upconing due to cyclic pumping by horizontal wells in freshwater lenses.

Received January 2015, accepted August 2015.

doi: 10.1111/gwat.12382

interface, Das Gupta and Gaikwad (1987) and Motz (1992) presented analytical solutions to calculate the critical pumping rate. Dagan and Bear (1968) presented analytical solutions for the rise of the interface due to pumping for a point well (i.e., axi-symmetric flow) and for an infinite horizontal well. Schmorak and Mercado (1969) used the analytical solutions of Dagan and Bear (1968) to determine the critical pumping rate of a point well in case of infinitely thick and confined freshwater and saltwater zones and to calculate the downward movement of the interface after the pumping stops.

Numerical models can also be used to quantify saltwater upconing. Numerical models based on the interface approach have, amongst others, been used by Das Gupta (1983) and Reilly et al. (1987a) to quantify interface upconing. In recent years, numerical models based on the miscible approach (e.g., SEAWAT version 4 [Langevin et al. 2007]) are used increasingly. However, the application of these numerical models to saltwater upconing problems is still often accompanied by relatively long simulation runtimes.

This article deals with the quantification of saltwater upconing below horizontal wells in freshwater lenses using analytical solutions as a computationally fast alternative to numerical simulations. The considered pumping regime is cyclic and representative of the extraction of fresh groundwater for irrigation during a dry half year. In coastal areas, horizontal wells are often preferred over vertical wells as they induce less saltwater upconing per volume of extracted groundwater (Yeh and Chang 2013). Analytical solutions based on the interface approach and superimposed analytical solutions used to account for mixing are compared with numerical simulations based on the miscible approach. Three aspects are considered, that is, (1) cyclic pumping; (2) dispersion; and (3) horizontal wells with finite length in a finite domain (a freshwater lens). The first aspect is considered as only a few previous studies on saltwater upconing have dealt with cyclic pumping even though it is common when water is extracted for irrigation purposes. The second aspect is important because dispersion adversely affects the salinity of the pumped groundwater. Comparisons regarding the third aspect are presented because the analytical interface solutions of Dagan and Bear (1968) that were used in this paper were derived for an infinite domain, whereas in reality, both freshwater lenses and horizontal wells are finite, which can be simulated using numerical simulations. For all three aspects, analytical calculations and numerical simulations are compared for a wide range of hydrogeological parameters and pumping regimes during a dry half year.

The reader is encouraged to consult the Supporting Information section of this article. It contains some of the results of this study as well as background information on the analytical solutions, the parameter combinations that were used, the set-up of the numerical models, and a list of symbols.

Material and Methods

Two-Dimensional (2D) and Three-Dimensional (3D) Models

Cyclic pumping and dispersion were investigated by applying numerical simulations and analytical calculations to a two-dimensional (2D) model. In the 2D model, the length of the horizontal well and the horizontal extent are assumed to be infinite. A finite horizontal well in a finite domain was investigated using a three-dimensional (3D) model. SEAWAT (Langevin et al. 2007) was used for all the numerical simulations. Grid convergence tests were performed for the numerical simulations to make sure that numerical dispersion was kept to a minimum.

In the following sections and paragraphs up to the "Results" section, the 2D and 3D model approaches for the three aspects (i.e., cyclic pumping, dispersion, and a horizontal well with a finite length in a finite domain) are explained. The sections and paragraphs also describe how the numerical simulations and analytical calculations were applied to these models and which parameters were varied.

Cyclic Pumping (2D Model)

The 2D model that was used to investigate cyclic pumping is shown in Figure 1. The extent of the model domain is infinite in the horizontal x (L) direction with the origin of the x axis ($x = 0$) located at the well. In view of vertical symmetry at $x = 0$, only half of the model domain was considered. In the vertical z (L) direction, the domain is finite with thickness D (L). The z coordinate is 0 at the top and is positive upwards. Groundwater with a density ρ_f (M/L^3) of 1000 kg/m^3, which is referred to in this article as "fresh" groundwater, is situated on top of saline groundwater with a higher density ρ_s (M/L^3). The freshwater density corresponds with a salt concentration C (M/L^3) of 0 kg/m^3. In the saline groundwater with density ρ_s, the concentration is equal to C_s (M/L^3). The density of the groundwater varies linearly with concentration. The aquifer has a homogeneous porosity (n) and horizontal (κ_x) and vertical permeabilities (κ_z) (both [L^2]). The horizontal (K_x) and vertical (K_z) hydraulic conductivities (L/T) based on fresh groundwater are defined as:

$$K_x = \frac{\kappa_x \rho_f g}{\mu_f}, \quad K_z = \frac{\kappa_z \rho_f g}{\mu_f}, \tag{1}$$

in which g is the gravitational acceleration (L/T^2), and μ_f is the dynamic viscosity based on fresh groundwater (M/(L T)). Elastic storage (storage coefficient) accounts for the compressibility of the groundwater, and porous medium and phreatic storage (specific yield) is used to account for the drainage at the water table (Domenico and Schwartz 1990).

Initially, at time t (T) = 0, the fresh and the saline groundwater are at rest, and the hydraulic head h (L) at the top of the aquifer is 0 m. The depth of the interface between fresh and saline groundwater ζ (L) is where

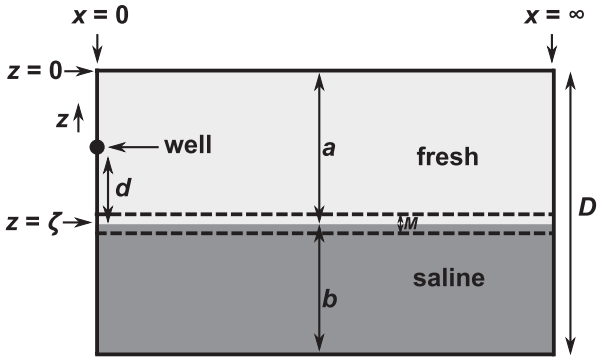

Figure 1. 2D cross-sectional conceptual model that was used in the analytical calculations and numerical simulations. The initial conditions (i.e., prior to pumping) are shown.

$C = 0.5C_s$. The initial thickness of the freshwater zone a (L) is defined as the distance between the initial interface depth and the top of the aquifer. The initial thickness of the saline groundwater zone b (L) is defined as the distance between the initial interface depth and the bottom of the aquifer. The well, which has a negligible screen length, is located at a vertical distance d (L) from the initial interface depth.

The initial thickness of the mixing zone M (L) around the interface ($C = 0.5C_s$), in which the vertical concentration is normally distributed (Gaussian), is defined as twice the distance between the interface and the depth at which the concentration equals $0.024C_s$, that is, two standard deviations from $0.5C_s$. A distinction is made between interface upconing (i.e., the interface approach) and salt water upconing (i.e., the miscible approach). Interface upconing is defined as the rise of the interface relative to the initial interface depth. Saltwater upconing is more generally defined than interface upconing, that is, saltwater upconing is the rise of the saline groundwater relative to its initial depth, regardless of its salinity (i.e., any concentration higher than freshwater).

A cyclic pumping regime is considered, which takes place during a period T_p (T) of 180 d. T_p represents a dry half year when irrigation is needed and consists of a number of cycles (n_{cyc}) in which fresh groundwater is pumped during a period T_{on} (T) followed by a period of no pumping T_{off} (T):

$$n_{cyc} = \frac{T_p}{T_{on} + T_{off}} \tag{2}$$

During T_{on}, fresh groundwater is pumped with a rate Q_d (L^2/T) (the pumping rate of the well per unit length of the well).

Numerical Simulations and Analytical Calculations

A 2D numerical model was constructed based on the model shown in Figure 1. A constant hydraulic head and constant concentration boundary condition was used at $x = 200$ m. Testing showed that, for the parameter variations that were considered, this was far enough to approximate an infinite domain. The hydraulic head at this boundary is 0 m at the top and hydrostatic downwards. The concentration at this boundary as well as the initial concentration was specified according to the initial thickness of the freshwater and saltwater zones (a and b) and the thickness of the mixing zone M.

The groundwater flow equation in the numerical simulations was solved using the PCG package. The advection part of the solute transport equation was solved using the MOC solver with a minimum number of 27 particles and a relatively low Courant number of 0.1. The dispersion part of the solute transport equation was solved using the GCG package. Detailed information about these three equations, the methods (packages) that were used to solve them, and the method of coupling variable density groundwater flow and solute transport can be found in the manual of SEAWAT (Langevin et al. 2007). A regular grid with a column width of 0.1 m and a layer thickness of 0.05 m was used.

The analytical interface solution presented by Dagan and Bear (1968) (their equation 43) using the transformation procedures for anisotropy presented by Bear and Dagan (1965) was applied to the model shown in Figure 1:

$$\zeta_{an}(x,t) = \frac{Q_d}{\delta\pi\sqrt{K_x K_z}} \int_0^\infty \frac{1}{\lambda} \frac{\cosh[\lambda(a-d)]}{\sinh(\lambda a)} \times \left[1 - \exp\frac{-\lambda t}{\frac{n}{\delta K_z}\coth(a\lambda) + \frac{n}{\delta K_z}\coth(b\lambda)}\right] \times \cos\left(\lambda x\sqrt{\frac{K_z}{K_x}}\right) d\lambda - a, \tag{3}$$

where ζ_{an} (L) is the analytically calculated depth of the interface, δ is defined as:

$$\delta = \frac{\rho_s - \rho_f}{\rho_f}, \tag{4}$$

and λ is the variable of integration. The superposition principle was used for cyclic pumping. For more information about this superposition procedure, the reader is asked to refer to the Supplemental Information. This also contains some background theories and a brief derivation of Equation 3.

An important aspect of Equation 3 is that it should only be used up to a certain degree of interface upconing. This is related to the method of small perturbations that Dagan and Bear (1968) used for the derivation. Dagan and Bear (1968) recommended using Equation 3 for cases where the interface upconing is less than 1/3 d, based on comparison with laboratory experiments. The dimensionless interface upconing d_ζ is defined as the analytically calculated interface upconing divided by d.

Parameter Variations and Definitions

The analytical calculations were compared with numerical simulations for various parameter combinations. The parameters T_p (180 d), n (0.3), a (12 m), b (18 m), d (7 m), and ρ_f (1000 kg/m^3) were kept constant as they were considered irrelevant or superfluous.

Table 1
Variation of Parameters in the 2D Model to Investigate Cyclic Pumping and Dispersion

Parameter	Variations	Units
Q_{tot} (18)	36, 54, 72, 80, 98	m^3/m
n_{cyc} (90)	180, 45, 30, 10, 1	—
Q_d (0.2)	20.0, 4.0, 2.0, 0.4, 0.16, 0.13, 0.11	$m^3/(m/d)$
K_x (10)	1, 5, 50, 100	m/d
K_x/K_z (1)	2.0, 5.0	m/d
C_s (35)	17.5, 8.25	kg/m^3
α_L (0.1)	0.01, 1.0	m
S_s (1E-5)	0	m^{-1}
S_y (0.15)	0	—
M (0)	1.4, 2.8	m

As certain parameters are related, a complete overview of all parameter combinations is given in the Supporting Information of this paper. Values between parentheses denote the reference values. The reference values for T_{on} and T_{off} are both 1 d. The storage parameters were only varied in the numerical simulations.

The molecular diffusion coefficient (D_m [L^2/T]) and the transverse dispersivity (α_T [L]) in the numerical simulations were 8.64E – 5 m^2/d and α_L/10 m, respectively. The influence of the parameters Q_{tot} (the total amount of extracted fresh groundwater during T_p [L^3]), n_{cyc}, Q_d, K_x, K_x/K_z, C_s, and α_L (the longitudinal dispersivity [L]) was investigated with respect to a set of reference parameters (Table 1). In addition to these parameters, the influence of the specific storage (S_s [L^{-1}]) and specific yield (S_y [–]) parameters was also investigated using numerical simulations as in Equation 3, it is assumed that the aquifer and groundwater are both incompressible.

The difference in the numerically simulated interface depth $\zeta_{num}(x, t)$ (L) and the analytically calculated interface depth $\zeta_{an}(x, t)$ (L) was calculated right below the well at the end of the pumping period ($t = T_p$). This difference is referred to as ε_ζ (L) and was calculated using:

$$\varepsilon_\zeta = \zeta_{an}\left(0, T_p\right) - \zeta_{num}\left(0, T_p\right) \quad (5)$$

In the Results section, ε_ζ is shown for each simulation using the parameter combinations listed in Table 1.

Dispersion (2D Model)

Numerical Simulations and Analytical Calculations

As Equation 3 is based on the interface approach, an analytical solution was superimposed on Equation 3 to account for dispersion. In this approach, which was based on the one used by Schmorak and Mercado (1969), mixing takes place by longitudinal dispersion due to the (cyclic) movement of the interface. It is thereby assumed that the saltwater upconing is governed by vertical flow (advection) and longitudinal dispersion, so mixing due to diffusion and transversal dispersion are neglected. In addition, it is assumed that the pore water velocity in the vertical does not vary (i.e., that it is equal to the velocity of the interface) and that the vertical concentration distribution around ζ is normally distributed. The same numerical simulations and analytical calculations that were used to investigate cyclic pumping were used to investigate the dispersion aspect.

The following equation was used to calculate zC_{an} (L), the analytically calculated depth of a concentration C:

$$zC_{an}(x, t, C) = \zeta_{an}(x, t) + 2\sqrt{\alpha_L(\eta + |s|)}\,\mathrm{erfc}^{-1}\left(2\frac{C}{C_s}\right). \quad (6)$$

$|s|$ (L) is the total travelled distance of the analytically calculated interface ζ_{an} after time t. $|s|$ can be calculated using Equation 3. η (L), the equivalent travelled distance of the interface, is defined as:

$$\eta(M, \alpha_L) = \frac{\left(\frac{0.5M}{2\mathrm{erfc}^{-1}(0.048)}\right)^2}{\alpha_L} \quad (7)$$

η was derived by calculating $|s|$ in Equation 6 using $C/C_s = 0.024$ (refer the definition of the initial width of the mixing zone M) and using the corresponding values of ζ_{an} and zC_{an}. It represents the width of the mixing zone in the form of the equivalent travelled distance of the interface. More details on this procedure, including derivations of Equations 6 and 7, are given in the Supporting Information section.

Parameter Variations and Definitions

Using the parameter combinations of the 2D model (Table 1 and Figure 1), the numerical and analytical results of two concentration values were analyzed:

$$C_{1\sigma} = 0.16C_s$$
$$C_{2\sigma} = 0.024C_s \quad (8)$$

$C_{1\sigma}$ and $C_{2\sigma}$ (both M/L^3) are the concentrations at one standard deviation and two standard deviations from the mean concentration ($0.5C_s$), respectively. The reference value of C_s is equal to 35 kg/m^3 and represents the total dissolved solids in ocean water. $C_{2\sigma}$ is then equal to 0.84 kg/m^3, which is representative of the drinking water standard (WHO 2011).

$C_{1\sigma\text{-an}}(x,t)$ and $C_{1\sigma\text{-num}}(x,t)$ are defined as the concentration $C_{1\sigma}$ in the analytical calculations (i.e., using Equation 6 with $zC_{an}(x, t, C_{1\sigma})$) and numerical simulations, respectively, and $zC_{1\sigma\text{-an}}(x,t)$ and $zC_{1\sigma\text{-num}}(x,t)$ are their corresponding depths. In a similar way, $C_{2\sigma\text{-an}}$, $C_{2\sigma\text{-num}}$, $zC_{2\sigma\text{-an}}$, and $zC_{2\sigma\text{-num}}$ are defined with respect to $C_{2\sigma}$. $\varepsilon_{1\sigma}$ (L) and $\varepsilon_{2\sigma}$ (L) are defined as the difference in the analytically calculated and numerically simulated depths of $C_{1\sigma}$ and $C_{2\sigma}$, right below the well at the end of the pumping period T_p:

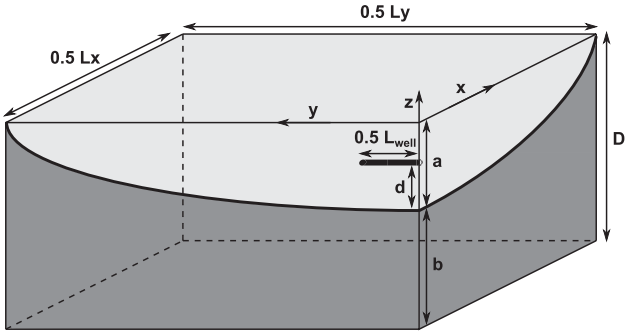

Figure 2. Overview of the 3D conceptual model prior to pumping. z is positive upwards. The light grey area shows the freshwater lens at the end of the initialization period. Note that the mixing zone between fresh and saline groundwater is not shown.

$$\varepsilon_{1\sigma} = zC_{1\sigma-\mathrm{an}}\left(0, T_\mathrm{p}\right) - zC_{1\sigma-\mathrm{num}}\left(0, T_\mathrm{p}\right),$$
$$\varepsilon_{2\sigma} = zC_{2\sigma-\mathrm{an}}\left(0, T_\mathrm{p}\right) - zC_{2\sigma-\mathrm{num}}\left(0, T_\mathrm{p}\right) \qquad (9)$$

In the Results section, $\varepsilon_{1\sigma}$ and $\varepsilon_{2\sigma}$ are shown for each simulation using the parameter combinations listed in Table 1.

Horizontal Wells with a Finite Length in a Finite Domain (3D Model)

Numerical simulations and analytical solutions were applied to a 3D model to investigate the finite length of both the horizontal well and the domain. In Figure 2, a quarter of this model is shown as the model is symmetrical along the x and y axes. Prior to pumping (in the initialization period), a freshwater lens is present in a finite domain with horizontal length L_x (L) and L_y (L) and thickness D. The freshwater lens terminates at the boundaries $x = 0.5L_x$ and $y = 0.5L_y$. The outflow level at the boundaries is equal to 0 m. Inflow can take place along the total vertical depth at the boundaries with a density ρ_s and corresponding concentration C_s. The vertical pressure distribution at the boundaries is hydrostatic.

The thickness of the freshwater lens in the initialization period varies due to natural recharge at the top of the total model area during a period T_rch (T) followed by a period T_dry (T), in which there is no natural recharge. T_rch has a length of 180 d in which the recharge rate (N [L/T]) is constant (0.002 m/d). The length of T_dry is also 180 d. The freshwater lens is in dynamic equilibrium, that is, the thickness of the freshwater lens is constant at the end of successive periods T_rch.

The end of the T_rch period is the initial condition for a period T_p of 180 d where cyclic pumping takes place. The well has a finite horizontal length L_well (L). Similar to the 2D model, during T_on, pumping takes place, whereas during T_off, there is no pumping. The pumping rate of the well during T_on is Q (L^3/T). An important assumption in the 3D model is that the discharge along the horizontal well is constant, so the frictional head losses in the well and the flow pattern around the well do not influence the inflow along the well. The well is located in the centre of the freshwater lens and oriented in the direction of the y-axis, the longest axis. The initial thickness of the freshwater and saltwater zones (a and b) and the thickness of the mixing zone M are considered at the centre of the horizontal well.

Numerical Simulations and Analytical Calculations

A 3D numerical model was constructed based on the model shown in Figure 2. The set-up of this numerical model is described in the Supplemental Information section. In the analytical calculations, the initial condition (i.e., the freshwater lens) was not simulated, but an infinite horizontal domain was assumed. The finite horizontal well was simulated by superposition of point sinks along the length of the well. This procedure is briefly explained in the Supporting Information section. For further details, the reader is referred to Reilly et al. (1987b) and Langseth et al. (2004). The following equation was used for each point sink:

$$\zeta_\mathrm{an}(r,t) = \frac{Q}{\delta 2\pi\sqrt{K_x K_z}} \int_0^\infty \frac{\cosh\left[\lambda\left(a-d\right)\right]}{\sinh\left(\lambda a\right)} \times \left[1 - \exp\frac{-\lambda t}{\frac{n}{\delta K_z}\coth\left(a\lambda\right) + \frac{n}{\delta K_z}\coth\left(b\lambda\right)}\right] \times J_0\left(\lambda r\sqrt{\frac{K_z}{K_x}}\right)\mathrm{d}\lambda - a \qquad (10)$$

J_0 is a Bessel function of the first kind (order zero), and r (L) is the horizontal radial distance from the well. This equation is based on equation 69 of Dagan and Bear (1968). Dagan and Bear derived this equation in a similar way as Equation 3, but it was used for a cylindrical, axisymmetric infinite domain with a vertical rotation axis at the location of the well. As this analytical solution was also derived using a perturbation approximation, it is subjected to the same applicability condition as Equation 3. The Supporting Information section provides background information on Equation 10.

Parameter Variations and Definitions

For the comparison of the 3D numerical simulations with the analytical calculations, saltwater upconing during the period T_p was analyzed. Similar to the 2D comparisons, reference parameters were chosen (Table 2), and some parameters were varied. However, fewer parameters were varied due to the computational effort of the numerical simulations. Most of parameters are equal to the reference values in the 2D model; the exceptions are shown in Table 2.

The reference parameter values result in a dimensionless, analytically calculated interface upconing (d_ζ) below 1/3. Variations of Q_tot were used to investigate the salinity of the water in the well in case d_ζ is closer or equal to 1/3. In addition, the length of the well was increased to investigate the influence of the finite domain (Table 2).

Table 2
Reference Parameters and Variations in the 3D Model

Parameter	Value	Units
Reference		
Q_{tot}	4500	m^3
Q_d	0.5	m^3/d
L_{well}	80	m
a	15.5	m
b	14.5	m
d	10	m
Variations		
Q_{tot}	12,000	m^3
L_{well}[1]	320, 640	m

Note that a and b were taken as the numerically simulated maximum thickness of the lens at the end of the initialization period.
[1]With an increase of the length of the well, the total extraction also increases, such that the extraction per unit length of the well remains 150 m^3/m. This value corresponds with $Q_{tot} = 12{,}000\ m^3$ and the reference length of the well $L_{well} = 80$ m (i.e., 12,000 m^3/80 m = 150 m^3/m).

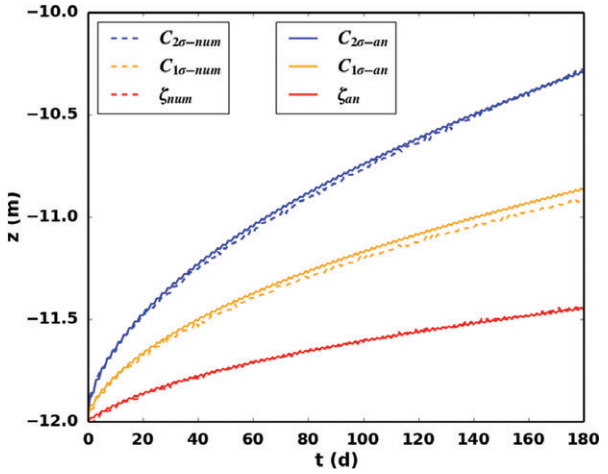

Figure 3. Analytically calculated depths of ζ_{an}, $C_{1\sigma\text{-an}}$, and $C_{2\sigma\text{-an}}$ (m) (solid lines) as well as the numerically simulated depths of ζ_{num}, $C_{1\sigma\text{-num}}$, and $C_{2\sigma\text{-num}}$ (m) (dashed lines) below the well using the reference parameters of the 2D numerical model. The pumping periods T_{on} and T_{off} are both 1 d.

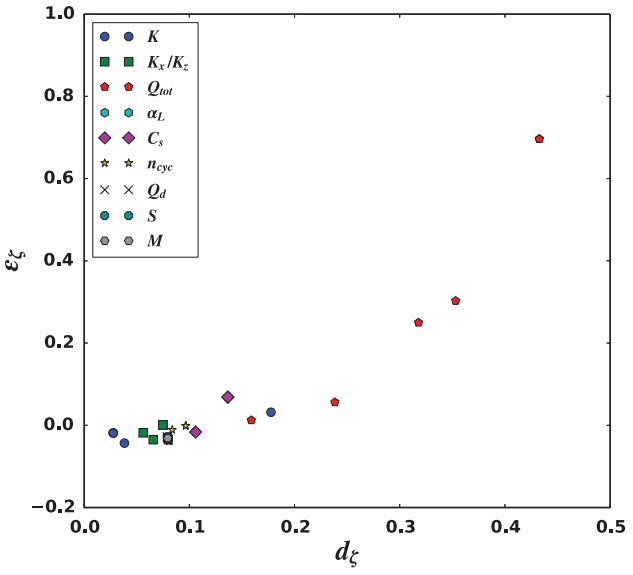

Figure 4. ε_ζ (m) vs. d_ζ for all parameter combinations (Table 1).

Results

Results of the 2D Numerical Simulation with the Reference Values and the Influence of Storage

In the Supporting Information section, the groundwater flow and mixing patterns of the numerical simulation using the reference parameters are described in detail. It is also shown that storage has a large influence on the groundwater flow patterns, but its influence on saltwater upconing is minimal. Furthermore, it is shown that below the well, longitudinal dispersion is dominant during cyclic pumping as the longitudinal dispersivity α_L was an order of magnitude larger than the transverse dispersivity and as the velocity vector and the concentration gradient below the well were parallel. This suggests that Equation 6 is appropriate to account for mixing by dispersion below the well.

In Figure 3, the numerically and analytically calculated depths of the interface below the well ($\zeta_{num}[0, t]$ and $\zeta_{an}[0, t]$, respectively) are shown throughout the pumping period T_p. It is clear that the differences are very small throughout T_p. The interface upconing is about 0.5 m at the end of the simulated period. This is within the applicability condition that was proposed by Dagan and Bear (1968). In the following two sections, the influence of the other parameter combinations on the difference between the analytical calculations and numerical simulations is discussed with respect to cyclic pumping and dispersion.

Cyclic Pumping (2D Model)

In Figure 4, the difference in the numerically simulated and analytically calculated interface depth right below the well at the end of the pumping period ε_ζ is plotted against the dimensionless, analytically calculated interface upconing d_ζ for all parameter combinations (Table 1). Most parameter combinations led to interface upconing within the applicability condition $d_\zeta < 1/3$. For these combinations, the errors in ε_ζ are small. For larger values of d_ζ, the difference between the analytical calculations and numerical simulations (i.e., the error ε_ζ) is significant. This threshold agrees well with previous results on non-cyclic interface upconing (Dagan and Bear 1968; Schmorak and Mercado 1969). ε_ζ is positive for large values of d_ζ, which indicates that in the analytical calculations, the interface upconing is underestimated.

Figure 4 reveals that the total volume of groundwater that is extracted (Q_{tot}) clearly has the largest influence on interface upconing and, hence, ε_ζ. Remarkably, the pumping rate and pumping period length (reflected by Q_d and n_{cyc}) have minimal influence (note that upon their variation Q_{tot} remains constant) even though their

variation is relatively large. In case n_{cyc} is equal to 1, the pumping period is 90 d and therefore the simulation is close to steady state. This indicates that for both cyclic pumping and with steady-state simulations, the interface upconing and ε_ζ are controlled by the total volume of the groundwater extracted (Q_{tot}).

Dispersion (2D Model)

In the case of the reference parameters, the difference between the numerical simulation and analytical calculation right below the well with respect to the concentration contours $C_{1\sigma}$ and $C_{2\sigma}$ are very small throughout T_p (Figure 3). Therefore, for these parameter combinations, it is appropriate to use Equation 6 to account for dispersion. In Figure 5, $\varepsilon_{1\sigma}$ and $\varepsilon_{2\sigma}$ (the difference between the numerical simulation and analytical calculation right below the well at the end of the period T_p with respect to the concentration contours $C_{1\sigma}$ and $C_{2\sigma}$, respectively) are plotted against d_ζ (the dimensionless interface upconing) for all parameter combinations. $\varepsilon_{1\sigma}$ and $\varepsilon_{2\sigma}$ are positive in case of significant interface upconing, similar to ε_ζ. This indicates that the depth of the concentration contours are underestimated in the analytical calculations. $\varepsilon_{1\sigma}$ and $\varepsilon_{2\sigma}$ are both higher than ε_ζ. This is because in Equation 7, it is assumed that the vertical flow distribution around the interface is constant, whereas in the numerical simulations, the vertical flow velocity varies spatially due to the radial flow resistance induced by the small well screen. Toward the well, the flow velocities increase inverse-proportionally, which also explains why $\varepsilon_{2\sigma}$ is higher than $\varepsilon_{1\sigma}$ at high values of d_ζ. Moreover, in case of a wide initial mixing zone M, the errors $\varepsilon_{1\sigma}$ and $\varepsilon_{2\sigma}$ are also high.

Similar to ε_ζ, parameter variations of the total amount of extracted groundwater (Q_{tot}) have the largest influence on $\varepsilon_{1\sigma}$ and $\varepsilon_{2\sigma}$. For Q_{tot}, $\varepsilon_{2\sigma}$ increases with increasing d_ζ (Figure 5) except for $d_\zeta = 0.35$ and $d_\zeta = 0.43$. In these cases, the numerically simulated $C_{2\sigma\text{-num}}$ has almost reached the well screen, and therefore, the difference with the analytically calculated $C_{2\sigma\text{-an}}$ decreases, which leads to a lower value of $\varepsilon_{2\sigma}$.

For some of the Q_d (pumping rate per unit length of the well) and n_{cyc} (number of pumping cycles) parameter variations, $\varepsilon_{1\sigma}$ and $\varepsilon_{2\sigma}$ are negative. The negative values indicate that dispersion is overestimated in the analytical calculations. The overestimation can be attributed to storage. The effect of the difference in storage between the numerical simulation and the analytical calculation is that saltwater upconing in the analytical calculations is higher than in the numerical simulation if the pumping rate is high (as is the case in some of the Q_d and n_{cyc} parameter variations). In case the pumping rate is high and no storage is simulated (see Table 1), $\varepsilon_{1\sigma}$ and $\varepsilon_{2\sigma}$ are both positive. For the parameter combinations that are considered in this article, the effect of the storage on saltwater upconing is relatively small.

For all parameter combinations except for the variations in the concentration of the saline groundwater C_s, $C_{2\sigma}$ represented the drinking water standard. From Figure 5, it is clear that using Equations 3 and 6 to estimate the depth of the contour of the drinking water concentration below the well leads to substantial errors when d_ζ increases, which indicates a practical limitation of the analytical solutions to estimate the concentration in the well in case of substantial saltwater upconing. For the parameter combinations listed in Table 1, the numerically simulated concentration in the well ($Cwell_{num}$ [M/L^3]) was compared with the analytically calculated, dimensionless interface upconing (expressed as d_ζ). Q_{tot} was not varied but kept constant at a high value (108 m^3/m) to ensure that the salinity in the well at the end of the numerical simulations was higher than $C_{2\sigma}$ (approximately equal to the WHO drinking water limit). For the concentration of the saline groundwater C_s, an additional concentration value of 3.5 kg/m^3 was investigated. For the longitudinal dispersivitiy α_L, the highest value of 1.0 m was not considered as this value is not very realistic for the type of aquifers that are considered here.

In Figure 6, $Cwell_{num}$ is plotted against d_ζ at the end of every T_{on} ("pumping on") and T_{off} ("pumping off") period throughout T_p for the three values of the maximum concentration of the ambient saline groundwater (C_s). Remarkably, C_s has a minor influence on the degree of interface upconing (as calculated with the analytical solution) at which the WHO drinking water limit is exceeded. The drinking water limit (0.84 kg/m^3) in the well is exceeded at an analytically calculated, dimensionless interface upconing $d_\zeta = 0.3$, 0.31, and 0.35 for $C_s = 35$, 17.5, and 3.5 kg/m^3, respectively. This can be explained by two effects that counteract each other. One effect is related to the absolute value of the maximum concentration C_s. The lower the C_s, the lower the salinity in the well. The other effect is related to the maximum groundwater density ρ_s. The lower the ρ_s, the faster saline groundwater flows toward the well. In case the largest value of the thickness of the mixing zone M is neglected, all parameter combinations yield a salinity lower than the drinking water in the well as long as $d_\zeta < 1/3$.

Horizontal Wells with a Finite Length in a Finite Domain (3D Model)

In Figure 7, the analytically and numerically determined values of the interface ζ and the concentration values $C_{1\sigma}$ and $C_{2\sigma}$ using the reference parameters just below the well are shown throughout T_p. In the analytical calculation, ζ_{an} is underestimated by about 0.35 m at the end of T_p. This is proportionally more than what was observed in the 2D model concept with the reference parameters, although still below the critical value of 1/3. The difference between the 2D and 3D results is attributed to the upward movement of the freshwater lens in a dry period (natural fluctuation of the lens), which increases the saltwater upconing.

In Figure 8, the analytical and numerical results using the same parameters as the reference values, but with a total volumetric extraction (Q_{tot}) of 12,000 m^3, are shown. As a result of the higher Q_{tot}, the saltwater

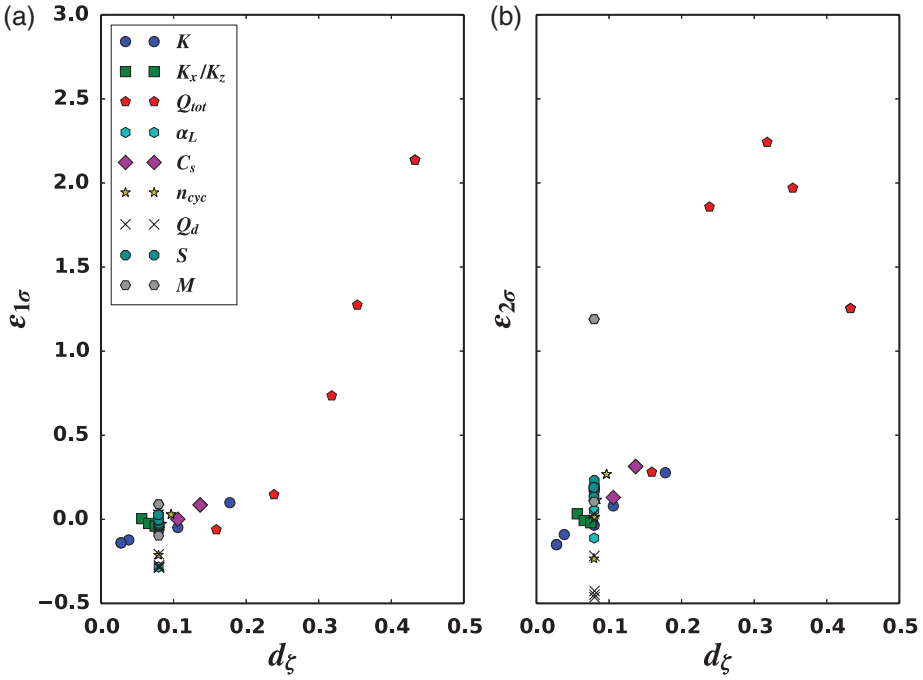

Figure 5. $\varepsilon_{1\sigma}$ (a) and $\varepsilon_{2\sigma}$ (b) and corresponding d_ζ for all parameter combinations and the end of T_p.

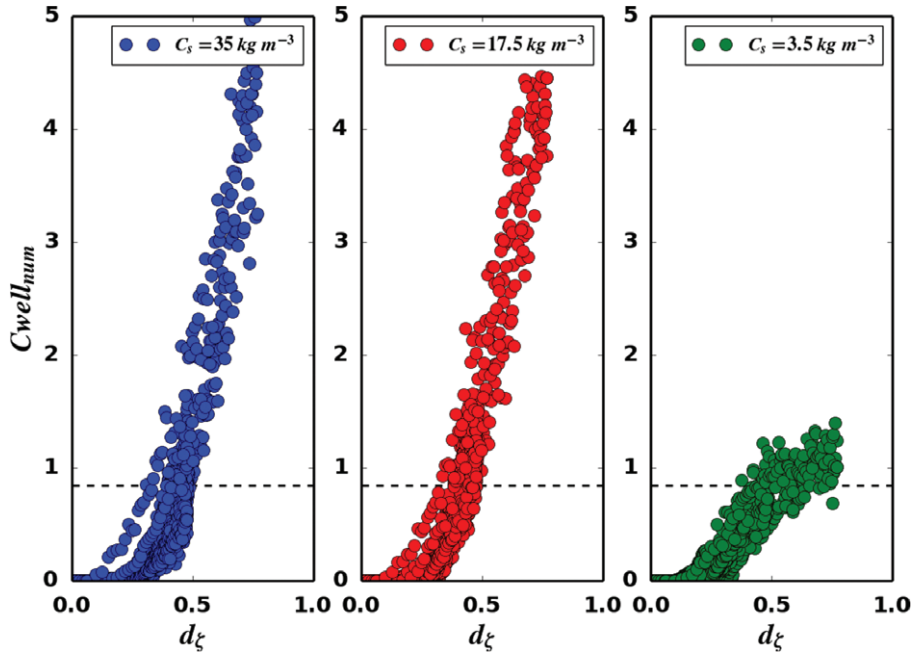

Figure 6. $C_{\text{well num}}$ (kg/m^3), the numerically simulated concentration in the well, vs. d_ζ, at the end of every periods T_{on} and T_{off} during T_p, for the three values of C_s. The horizontal dashed line indicates the WHO drinking water limit (0.84 kg/m^3).

upconing is larger than for the reference parameters. As expected, the differences between analytical calculations and numerical simulations with respect to ζ, $C_{1\sigma}$, and $C_{2\sigma}$ are also larger. For this value of Q_{tot}, the dimensionless, analytically calculated interface upconing d_ζ at the end of the total pumping period T_p is 0.28. The numerically simulated concentration in the well is 0.88 kg m^{-3}, which is slightly higher than the drinking water limit of 0.84 kg/m^3. The drinking water limit is exceeded at $d_\zeta = 0.27$. In the 2D numerical simulations, the concentration in the well did not exceed the drinking water limit as long as the corresponding d_ζ was less than 0.3. This difference is again attributed to the half-yearly variation of the thickness of the freshwater lens.

In Figure 9, the three variations of the length of the well L_{well} are shown at the end of T_p. In case $L_{well} = 80$ m, both the analytical calculation and numerical simulation show the largest interface upconing below the centre of

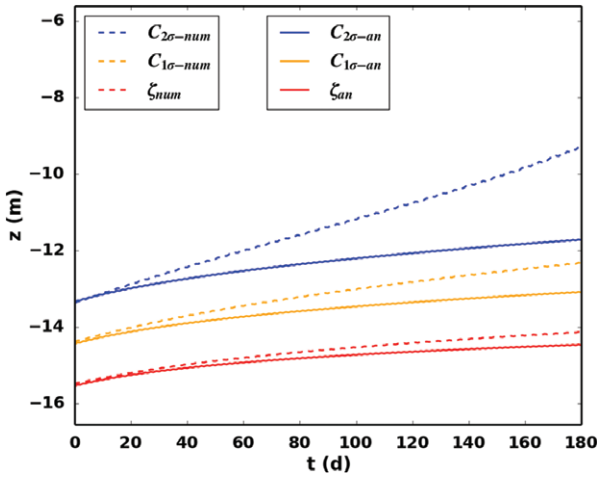

Figure 7. Analytically calculated depths of ζ_{an}, $C_{1\sigma\text{-an}}$, and $C_{2\sigma\text{-an}}$ (m) (solid lines) as well as the numerically simulated depths of ζ_{num}, $C_{1\sigma\text{-num}}$, and $C_{2\sigma\text{-num}}$ (m) (dashed lines) below the centre of the well using the reference parameters of the 3D conceptual model.

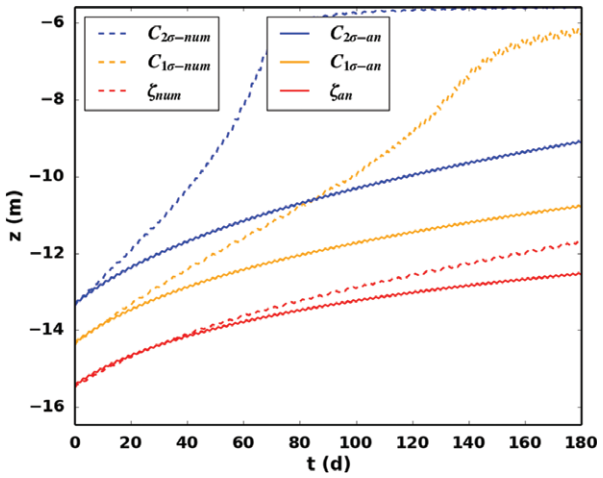

Figure 8. Analytically calculated depths of ζ_{an}, $C_{1\sigma\text{-an}}$, and $C_{2\sigma\text{-an}}$ (m) (solid lines) as well as the numerically simulated depths of ζ_{num}, $C_{1\sigma\text{-num}}$, and $C_{2\sigma\text{-num}}$ (m) (dashed lines) below the centre of the well using the reference parameters of the 3D conceptual model, but with a Q_{tot} of 12,000 m^3.

the well and show that the interface upconing decreases towards the outer end of the well. This is attributed to the difference in flow pattern between the centre and the outer end of the well, which induces less drawdown of the water table and less saltwater upconing at the outer end of the well, compared to the centre of the well. From the outer end of the well toward the end of the freshwater lens, the difference in ζ between the analytical and numerical results increases, which is related to the finite numerical model (i.e., the freshwater lens) and the analytical solution based on an infinite domain.

In case $L_{well} = 320$ m, the analytical and numerical results show the same similarities and differences when compared with $L_{well} = 80$ m except that the interface upconing is larger as well as constant over a significant length of the well. The reason for this is that in case $L_{well} = 320$ m, the flow pattern at the outer ends does not influence (i.e. reduce) the drawdown and the saltwater upconing at the centre, in contrast to the case where $L_{well} = 80$ m. For $L_{well} = 640$ m, the numerical simulation shows that the largest saltwater upconing occurs at the outer end of the horizontal well, not at the centre. The reason for this is that in the numerical simulation, the freshwater lens decreases in the direction of the edges, and therefore, the distance between the depth of the well and the initial depth of the interface (i.e., the distance d) decreases. Based on these results, it can be expected that the analytical solution gives appropriate indications of saltwater upconing in case the initial distance between the interface and the well d does not vary significantly below the horizontal well. In case $L_{well} = 320$ m, the numerically simulated concentration in the well did not exceed the drinking water limit in case $d_\zeta = 0.27$ (the threshold that was found in case $L_{well} = 80$ m).

Discussion

Regarding the cyclic pumping regimes presented in this article, it is expected that the analytical solutions of Dagan and Bear (1968) also closely resemble numerical simulations for other (e.g., more irregular) pumping regimes than that were analyzed, provided that the dimensionless interface upconing remains below 1/3. This limitation of a cyclic pumping regime is in line with previous studies that have dealt with steady-state pumping (Dagan and Bear 1968; Schmorak and Mercado 1969), where this limitation has been referred to as "critical rise." For brevity, a discussion on the concept of critical rise is given in the Supporting Information section. Below the critical rise, the analytical solutions can be a computationally fast alternative to numerical models for calculating the interface upconing.

Regarding dispersion, mixing below the well was dominated by longitudinal dispersion during cyclic pumping as the longitudinal dispersivity was an order of magnitude larger than the transverse dispersivity (similar as found or assumed in many previous studies, for example, Gelhar et al. (1992) and Janković et al. (2009)) and as the velocity vector and the concentration gradient below the well were parallel. Unfortunately, for estimating the concentration in the well, superimposing the effect of longitudinal dispersion on the analytical interface solutions was inappropriate. This has also been noted in previous studies (Schmorak and Mercado 1969; Wirojanagud and Charbeneau 1985) but has not been analyzed as in this study.

For the analytical calculation of saltwater upconing below horizontal wells with a finite length in freshwater lenses, the natural (seasonal) variation of the thickness of the freshwater is not taken into account. The results of the 3D model showed that the drinking water limit in the numerical model was exceeded at an analytically calculated, dimensionless interface upconing (d_ζ) of 0.27, a lower value than what was obtained in the 2D results

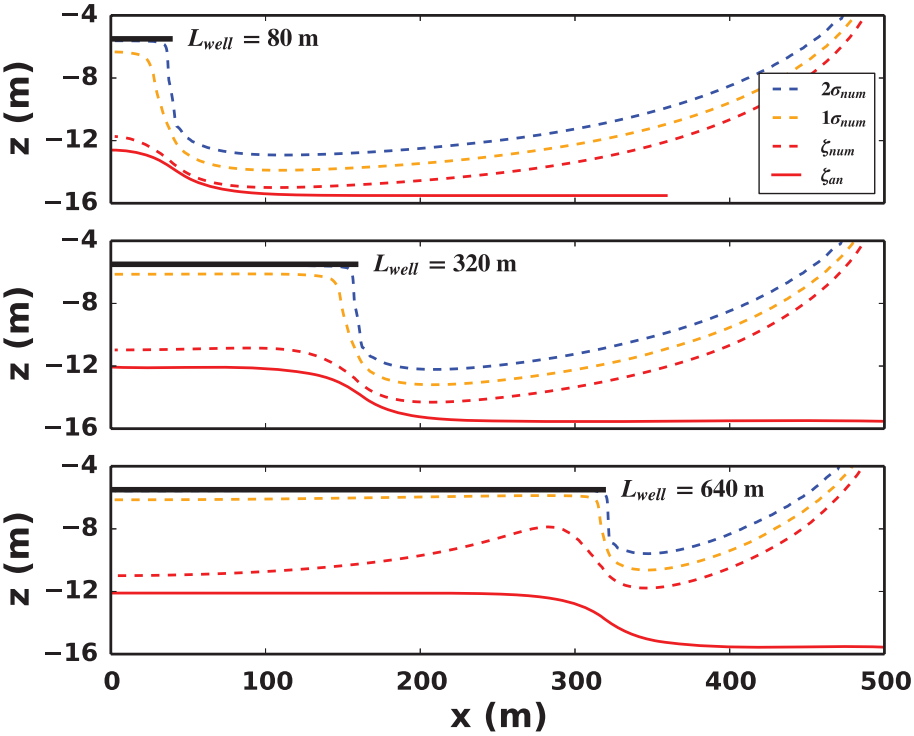

Figure 9. Analytically calculated depths of ζ_{an}, $C_{1\sigma\text{-an}}$, and $C_{2\sigma\text{-an}}$ (m) (solid lines) as well as the numerically simulated depths of ζ_{num}, $C_{1\sigma\text{-num}}$, and $C_{2\sigma\text{-num}}$ (m) (dashed lines) below the well using three different lengths of the well (L_{well}) where the extraction per unit length of the well is equal to 150 m^3/m. Note the values of L_{well} hold for the total length of the well, but that (given the symmetry) only half of the well is indicated. The centre of the well is located at $x = 0$.

(0.3). As the effect of the natural variation of the freshwater lens was not investigated in great detail, it is advised here that for maintaining a salinity of the pumped groundwater lower than that of the drinking water limit, d_ζ should be kept relatively small (e.g., 0.25). However, it should be noted here that this holds only for one half year when irrigation is needed, which is an important limitation of this study. The differences between analytical solutions and the numerical models for the long term are expected to depend strongly on the groundwater recharge. This aspect is left for further study.

For the analytical calculation of saltwater upconing due to pumping by a horizontal well with a finite extent, it was assumed that the frictional head losses (Rushton and Brassington 2013) within the horizontal well are negligible. In case the head losses are significant, however, the inflow along the horizontal well varies significantly. Moreover, even if the frictional head loss in the horizontal well is negligible, the inflow along the horizontal well varies as the flow pattern at the edges of well is different than in the centre of the well. These issues are left for further study. It should be noted here that if the variation of inflow along the well is calculated or measured, the analytical solution and the superposition principle can account for the variable inflow along the well by giving each point sink along the horizontal well an extraction rate according to the calculated inflow along the well.

Conclusions

Comparisons between analytical solutions and numerical simulations for the quantification of saltwater upconing below horizontal wells in freshwater lenses have indicated that under certain conditions, the analytical solutions can be used as a computationally fast alternative to numerical simulations. The comparisons were made regarding three aspects: (1) cyclic pumping; (2) dispersion; and (3) finite horizontal wells in a finite domain (a freshwater lens). Regarding cyclic pumping, elastic and phreatic storage (which are not taken into account in the analytical solutions) do not significantly influence the upconing of the interface. Furthermore, the analytical calculations based on the interface approach compare well with numerical simulations as long as the dimensionless interface upconing is below 1/3, which is in line with previous studies on steady pumping. Regarding dispersion, superimposing an analytical solution for mixing by dispersion below the well over an analytical solution based on the interface approach is appropriate in case the vertical flow velocity around the interface is nearly constant but should not be used for estimating the salinity of the pumped groundwater. Analytical calculations of a finite horizontal well are appropriate in case the distance between the horizontal well and the initial interface does not vary significantly along the well and in case the natural fluctuation of the freshwater lens is small. For maintaining a low salinity in the well during

a dry half year, the dimensionless, analytically calculated interface upconing should stay below 0.25.

Authors' Note

The authors have no conflict of interest to disclose.

Acknowledgments

This work was carried out within the Dutch "Knowledge for Climate" program. The numerical simulations were pre-processed and post-processed using the Python library FloPy (https://code.google.com/p/flopy/).

Supporting Information

Additional Supporting Information may be found in the online version of this article:

Appendix S1. Electronic supplement for "Saltwater upconing due to cyclic pumping by horizontal wells in freshwater lenses."

References

Bear, J., A.H.D. Cheng, S. Sorek, D. Ouazar, and I. Herrera. 1999. *Seawater Intrusion in Coastal Aquifers. Concepts, Methods and Practices*. Dordrecht, The Netherlands: Kluwer Academic Publishers.

Bear, J., and G. Dagan. 1965. The relationship between solutions of flow problems in isotropic and anisotropic soils. *Journal of Hydrology* 3: 88–96.

Bower, J.W., L.H. Motz, and D.W. Durden. 1999. Analytical solution for determining the critical condition of saltwater upconing in a leaky artesian aquifer. *Journal of Hydrology* 221: 43–54.

Custodio, E., and G.A. Bruggeman. 1987. Groundwater problems in coastal areas: A contribution to the International Hydrological Programme. Studies and reports in hydrology, vol. 45. Paris, France: UNESCO.

Dagan, G., and J. Bear. 1968. Solving the problem of local interface upconing in a coastal aquifer by the method of small perturbations. *Journal of Hydraulic Research* 6: 15–44.

Das Gupta, A., and V.P. Gaikwad. 1987. Interface upconing due to a horizontal well in unconfined aquifer. *Ground Water* 25, no. 4: 466–474.

Das Gupta, A. 1983. Steady interface upconing beneath a coastal infiltration gallery. *Ground Water* 21, no. 4: 465–474.

Domenico, P.A., and F.W. Schwartz. 1990. *Physical and Chemical Hydrology*. New York: John Wiley and Sons.

Garabedian, S.P. 2013. Estimation of salt water upconing using a steady-state solution for partial completion of a pumped well. *Ground Water* 51, no. 6: 927–934.

Gelhar, L.W., W. Welty, and K.W. Rehfeldt. 1992. A critical review of data on field-scale dispersion of aquifers. *Water Resources Research* 28, no. 4: 1955–1974.

Janković, I., D.R. Steward, R.J. Barnes, and G. Dagan. 2009. Is transverse macrodispersivity in three-dimensional groundwater transport equal to zero? A counterexample. *Water Resources Research* 45, no. 8: 1–10.

Langevin, C.D., D.T. Thorne Jr., A.M. Dausman, M.C. Sukop, and W. Guo. 2007. *SEAWAT Version 4: A Computer Program for Simulation of Multi-Species Solute and Heat Transport: U.S. Geological Survey Techniques and Methods Book 6* Chapter A22, 39. Reston, Virginia: U.S. Geological Survey.

Langseth, D.E., A.H. Smyth, and J. May. 2004. A method for evaluating horizontal well pumping tests. *Ground Water* 42, no. 5: 689–699.

Motz, L.H. 1992. Salt-water upconing in an aquifer overlain by a leaky confining bed. *Ground Water* 30, no. 2: 192–198.

Reilly, T.E., M.H. Frimpter, D.R. LeBlanc, and A.S. Goodman. 1987a. Analysis of steady-state salt-water upconing with application at Truro well field, Cape Cod, Massachusetts. *Ground Water* 25, no. 2: 194–206.

Reilly, T.E., L.O. Franke, and G.D. Bennett. 1987b. *The Principle of Superposition and Its Application in Ground-Water Hydraulics. U.S. Geological Survey Techniques of Water-Resources Investigations Book 3* Chapter B6. Denver, Colorado: U.S. Geological Survey.

Rushton, K.R., and F.C. Brassington. 2013. Significance of hydraulic head gradients within horizontal wells in unconfined aquifers of limited saturated thickness. *Journal of Hydrology* 492: 281–289.

Schmorak, S., and A. Mercado. 1969. Upconing of fresh water-sea water interface below pumping wells, field study. *Water Resources Research* 5, no. 6: 1290–1311.

Stuyfzand, P.J. 1996. Salinization of drinking water in the Netherlands: Anamnesis, diagnosis and remediation. In *Proceedings of the 14th Salt Water Intrusion Meeting, Malmö, Sweden*, June 16–21, Malmö, Sweden.

Werner, A.D., M. Bakker, V.E.A. Post, A. Vandenbohede, C. Lu, B. Ataie-Ashtiani, and C.T. Simmons. 2013. Seawater intrusion processes, investigation and management: recent advances and future challenges. *Advances in Water Resources* 51: 3–26.

WHO. 2011. Guidelines for drinking-water quality, 4th ed. http://www.who.int/water_sanitation_health/publications/2011/dwq_guidelines/en/ (accessed September 24, 2015).

Wirojanagud, B.P., and R.J. Charbeneau. 1985. Saltwater upconing in unconfined aquifers. *Journal of Hydraulic Engineering* 111, no. 3: 417–434.

Yeh, H.D., and Y.C. Chang. 2013. Recent advances in modeling of well hydraulics. *Advances in Water Resources* 51: 27–51.

Zhang, H., G.C. Hocking, and D.A. Barry. 1997. An analytical solution for critical withdrawal of layered fluid through a line sink in a porous medium. *The Journal of the Australian Mathematical Society. Series B. Applied Mathematics* 39: 271–279.